J Biomol NMR (2012) 52:277–282
DOI 10.1007/s10858-012-9608-7

NMR STRUCTURE NOTE

# The insect defensin lucifensin from *Lucilia sericata*

**Mads Kristian Erlin Nygaard · Anders Schou Andersen · Hans-Henrik Kristensen · Karen Angeliki Krogfelt · Peter Fojan · Reinhard Wimmer**

Published online: 10 February 2012


## Biological context

Today, the use of maggot debridement therapy has undergone a renaissance as it is increasingly being used when treating chronic wounds. However, it has also become a target in the search for new antibiotics as the disinfecting abilities of *L. sericata* maggots also apply to multidrug-resistant bacteria, such as methicillin-resistant *Staphylococcus aureus* (MRSA) (Kerridge et al. 2005). The wound healing properties of the larvae occurs mainly through debridement and disinfection (Dumville et al. 2009). The removal of bacteria occurs through ingestion and degradation of the bacteria, however, the larvae also produce excretions/secretions (ES) which confer reduction in the amount of especially Gram positive bacteria (Jaklic et al. 2008).

Recently a 40 residue antimicrobial peptide (lucifensin) has been found in various tissues and the extracellular secretion (ES) of *L. sericata*, isolated and sequenced (Čeřovský et al. 2009). It was found by studying radial diffusion assays (RDA) of fractions from reverse phase high-performance liquid chromatography (RP-HPLC) and size exclusion chromatography. The peptide has high sequence similarity with insect defensins from other insects. The sequences of insect defensins are highly conserved, especially the 6 cysteines which have the pairing Cys1–Cys4, Cys2–Cys5 and Cys3–Cys6 of which the first connects the loop and second $\beta$-strand while the two remaining pairs connect the $\alpha$-helix and first $\beta$-strand.

Sapecin from *Sarcophaga peregrina* (Hanzawa et al. 1990, PDB entry: 1L4V) and insect defensin A from *Phormia terranova* (Cornet et al. 1995, PDB entry: 1ICA) are two well studied insect defensins, for which the 3D structure has already been determined. Many of the studies have focused on elucidating the defensin-membrane interactions as these are believed to cause antimicrobial activity, which for insect defensins primarily is observed against Gram-positive bacteria. A study of the effect of insect defensin A on *Micrococcus luteus* revealed that the defensin permeabilized the cytoplasmic membrane leading to loss of cytoplasmic potassium, partial depolarization of the inner membrane and decrease in cytoplasmic ATP (Cociancich et al. 1993). It was proposed that the cause of these effects is a pore formation in the cytoplasmic membrane by defensin A oligomers. However, a recent study of the fungal defensin plectasin, which also has an insect defensin motif, showed that it had a bacterial killing mechanism which did not involve membrane permeabilisation (Schneider et al. 2010). Instead plectasin was found to target the cell wall precursor lipid II, which it binds to, thus inhibiting synthesis of cell walls. In the same study it was also found that lucifensin is able to bind to lipid II in a stoichiometric ratio and therefore possibly has two mechanisms of action.

M. K. E. Nygaard · P. Fojan
Institute for Physics and Nanotechnology, Aalborg University, Skjernvej 4A, 9220 Aalborg Ø, Denmark

A. S. Andersen · H.-H. Kristensen
Novozymes A/S, 2880 Bagsværd, Denmark

A. S. Andersen · K. A. Krogfelt
The Department of Microbiological Surveillance and Research, Statens Serum Institute, Ørestads Boulevard 5, 2300 Copenhagen S, Denmark

R. Wimmer (✉)
Department for Biotechnology, Chemistry and Environmental Engineering, Aalborg University, Sohngaardsholmsvej 49, 9000 Aalborg, Denmark
e-mail: rw@bio.aau.dk

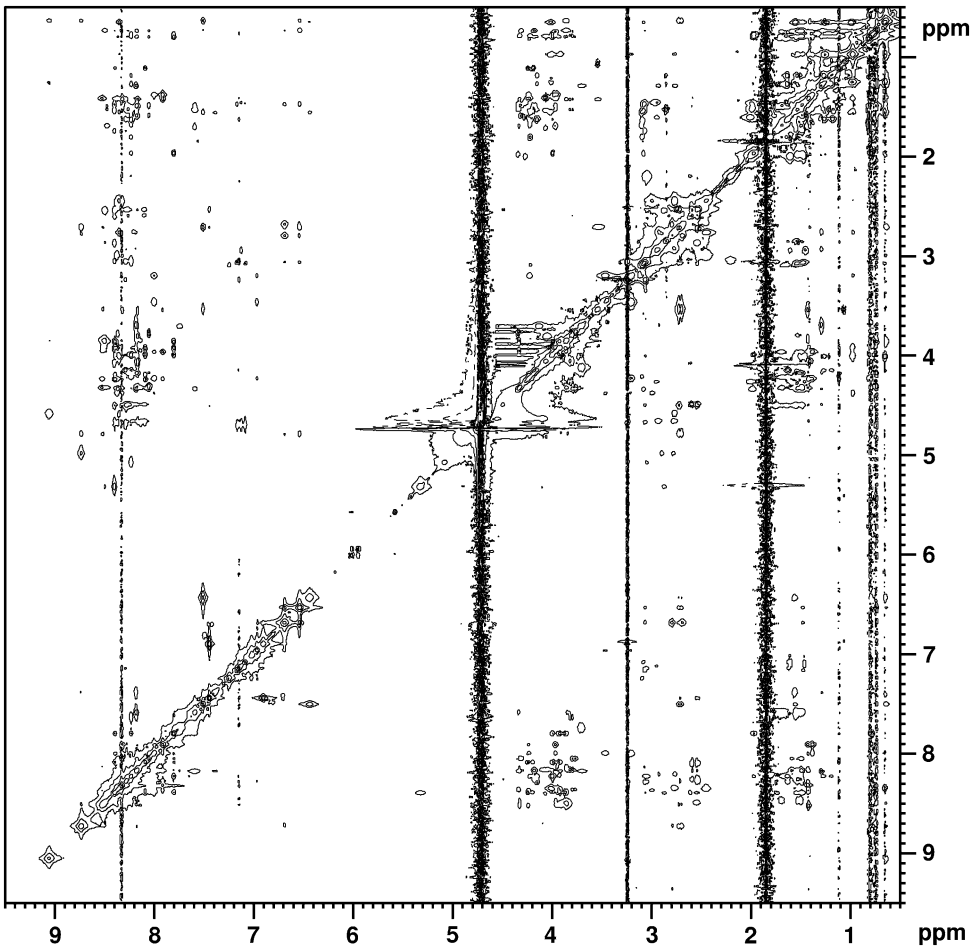


**Fig. 1** 800 MHz NOESY NMR spectrum used for structure determination. The mixing time was 120 ms, water suppression was achieved by Excitation Sculpting

## Methods and results

Lucifensin was expressed and purified according to (Andersen et al. 2010). A lyophilised sample of lucifensin was resuspended in 0.1% acetic acid, adjusted to pH 5.0 with NaOH, added 5% $D_2O$ and loaded into a 5 mm Shigemi tube. The final concentration of lucifensin was found to be 2 mM using a NanoDrop 1000 Spectrophotometer (Thermo Scientific) and a calculated molar extinction coefficient of 1,865 L $mol^{-1}$ $cm^{-1}$ (ProtParam, expasy.org).

Two sets of NMR spectra were recorded on the sample, one at 10°C and one at 25°C. The spectra at 10°C were recorded using a BRUKER 600 MHz spectrometer with a 5 mm TXI(H/C/N) probe. TopSpin v. 1.3 was used for recording and processing NMR data. The following spectra were recorded at 10°C: $^{1}H$–$^{1}H$-TOCSY with 90 ms mixing time, $^{1}H$–$^{1}H$-NOESY with 75 ms mixing time and $^{13}C$-HSQC (at natural abundance). WATERGATE was used for water suppression. The spectra at 25°C were recorded using a BRUKER 800 MHz NMR spectrometer equipped with a TCI cryogenic probe. TopSpin v. 2.1 was used for recording and processing NMR data. The following spectra were recorded at 25°C: $^{1}H$–$^{1}H$-TOCSY with 90 ms mixing time, $^{1}H$–$^{1}H$-NOESY with 120 ms mixing time and $^{1}H$–$^{13}C$-HSQC at natural abundance. Excitation sculpting was used for water suppression. The 800 MHz NOESY spectrum is shown in Fig. 1.

The individual spin systems were assigned in the $^{1}H$–$^{1}H$-TOCSY spectrum using CARA v. 1.8.4 with the aid of the COSY and HSQC spectra. All backbone signals were assigned except for $H^{N}$ of Cys30. Subsequently, NOE cross-peaks were identified and assigned in the $^{1}H$–$^{1}H$-NOESY spectra using CARA v. 1.8.4 (Keller 2004). The NOE-peak intensities were found by integrating the peaks in NEASY. The NOE cross-peak intensities were then converted to distance restraints in the CYANA v. 2.1 software (López-Méndez and Güntert 2006). $C^{\alpha}$ and $C^{\beta}$ chemical shifts were obtained from the HSQC spectra and used to calculate backbone torsion angle restrains using the program TALOS+ (Shen et al. 2009). On the basis of the distance constrains and angle restrains the structure of lucifensin was calculated using CYANA v 2.1. The structure was calculated from 100 random starting conformers from which the 20 with the lowest target

**Table 1** Structural statistics of lucifensin

| | Lucifensin before energy-minimization | Lucifensin after energy-minimization |
|---|---|---|
| NOE derived distance constraints | | |
| Intra-residue | 169 | |
| Sequential ($i - j = 1$) | 99 | |
| Medium-range ($1 < i - j < 5$) | 41 | |
| Long-range | 55 | |
| Total distance constraints | 364 | |
| TALOS+ derived dihedral angle restraints | | |
| $\varphi$ Angles | 21 | |
| $\Psi$ Angles | 21 | |
| Total number of dihedral angle restraints | 42 | |
| CYANA residual target function (Å$^2$) | 0.30 ± 0.06 | |
| Average energy results (kJ/mol) | | |
| Total energy | | −15,135 ± 53 |
| Restraint violation energy | | 3.9 ± 2.1 |
| Distance restraints | | 3.9 ± 2.1 |
| Dihedral angle restraints | | 0.1 ± 0.0 |
| Force field energy | | −15,139 ± 55 |
| Internal solute energy | | −8,669 ± 25 |
| Electrostatic solv. energy | | −6,279 ± 69 |
| Van der Waals solv. energy | | −194 ± 7 |
| RMSD for residue 2–39 | | |
| Average backbone ($N + C^{\alpha} + C$) | 0.98 ± 0.45 A | 0.25 ± 0.09 A |
| Average heavy atoms | 1.40 ± 0.44 A | 0.32 ± 0.08 A |
| RMSD for residue 14–39 | | |
| Average backbone ($N + C^{\alpha} + C$) | 0.36 ± 0.06 A | 0.21 ± 0.08 A |
| Average heavy atoms | 1.00 ± 0.08 A | 0.29 ± 0.07 A |
| Residual violations | | |
| No of NOE constraint violations > 0.1 Å | | 0.65 pr. structure |
| Maximum NOE violation | | 0.13 Å |
| No of Dihedral angle restraint violations > 5° | | 0.25 pr. structure |
| Ramachandran plot statistics | | |
| Residues in favoured regions | 80.5% | 87.0% |
| Residues in additional allowed regions | 18.9% | 13.0% |
| Residues in generally allowed regions | 0.0% | 0.0% |
| Residues in disallowed regions | 0.6% | 0.0% |

function values were chosen for energy minimization in YASARA. The statistics from the structure calculation are listed in Table 1.

The 20 structures were energy minimized with YASARA (Krieger et al. 2002) through two steps. First *in vacuo* with the YASARA force field (Krieger et al. 2009) and then second with water as explicit solvent using the particle mesh Ewald method (Essmann et al. 1995) and the YASARA force field. The statistics from the energy minimization are listed in Table 1.

Disulfide topology was initially left undefined in the structure calculation. However, the structure calculation quickly showed that only one disulfide topology was possible based on the observed NOEs. This topology is identical to the disulfide topology published earlier (Čeřovský et al. 2009). During further structure calculations, the disulfide topology was defined beforehand.

The bundle of 20 structures is shown in Fig. 2. From these structures it becomes obvious, that lucifensin has a characteristic insect defensin motif: a loop (residues 1–12), followed by an $\alpha$-helix (residues 13–23), a turn, a $\beta$-strand (residues 28–31), a turn and a $\beta$-strand (residues 34–38). In the structure, the cysteines follow the pairing pattern Cys3–

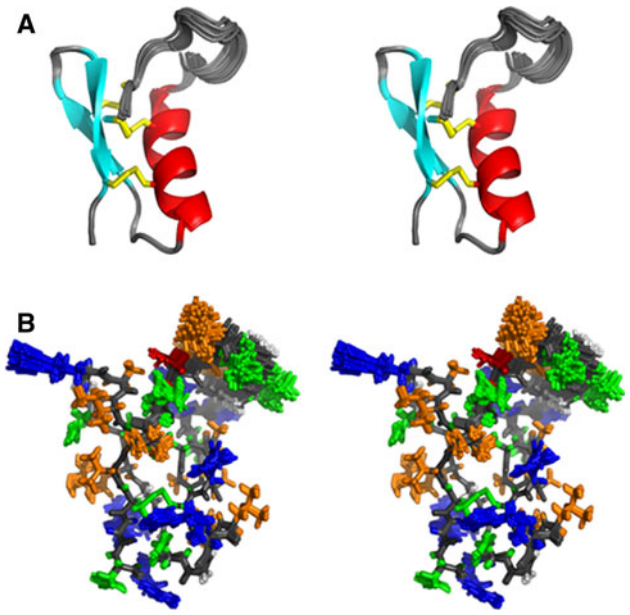


**Fig. 2** Stereo views of the bundle of 20 structures of lucifensin: **a** *cartoon* showing regular secondary structure elements and disulfide bridges; **b** *stick* representation with all side chains (*blue*: basic (including His), *red*: acidic, *green*: polar, *orange*: apolar, *grey*: backbone)

Cys30, Cys16–Cys36 and Cys20–Cys38. The 3D-structure of lucifensin can be classified as a CS$\alpha\beta$ (cysteine-stabilized $\alpha\beta$) fold.

The 20 structures coincide well. There is some structural flexibility in the two turns and at the N-terminus, and there is a larger flexibility in the loop region from residues 4–12. This is also reflected in the average backbone RMSD, which for residues 2–39 is 0.25 ± 0.09 Å, while for residue 14–39 it is 0.21 ± 0.07 Å. PROCHECK_NMR (Laskowski et al. 1996) was used to determine the distribution of $\varphi/\psi$ angles in the different regions of the Ramachandran plot. 87.0% of the residues were in the most favored regions, 13.0% were in additionally allowed regions and there were no residues in generously allowed or unfavorable regions. The $\varphi/\psi$ angles of residue 32, 33 and 34 (data not shown), which are involved in the turn between the two $\beta$-strands, show that the turn follows the characteristic and common 3:3 $\alpha_R\alpha_R\alpha_L$ turn and that it is a type I $\beta$-turn.

The hydrophobic and charged residues are highlighted in Fig. 2. Among the hydrophobic residues, only the cystines are located in the core of lucifensin while the rest is solvent exposed.

Atomic coordinates of lucifensin have been deposited at the Protein Data Bank (PDB ID 2lld). Assignment of NMR resonances has been deposited at the BioMagResBank (BMRB ID 18043).

## Discussion and conclusion

Lucifensin has a high sequence similarity of 90.0 and 87.5% with the two insect defensins sapecin (Hanzawa et al. 1990) and insect defensin A (Cornet et al. 1995), respectively. Also the tertiary structure of lucifensin is very similar to the structures of the two insect defensins. When performing pairwise structural alignment with the MUSTANGPP method (Konagurthu et al. 2006) implementation in YASARA, lucifensin and sapecin have an RMSD value of 1.41 Å (using $C^{\alpha}$ of residues 1–3, 5–8 and 13–40), while lucifensin and plectasin (Mygind et al. 2005, PDB entry 1ZFU) show an RMSD of 1.68 Å (using $C^{\alpha}$ of residues 1–8 and 13–40).

The high sequence similarity suggests that lucifensin has the same mode of action as reported for sapecin (Takeuchi et al. 2004) and insect defensin A (Cociancich et al. 1993).

In the study of sapecin, changes in NMR chemical shifts were examined and a model was proposed for sapecin in which it forms membrane pores by formation of oligomers. In the proposed model, the hydrophobic residues of the loop and α-helix of sapecin are buried in the phospholipid membrane. Furthermore, it was also found that the two charged residues Asp4 and Arg23 were of high importance for the pore forming ability. These residues are highly conserved in the sequences of insect defensins (Bulet et al. 1992), which further supports their importance for the mechanism of action. When comparing the sequence of lucifensin to those of sapecin and insect defensin A (Fig. 3), it is seen that they are completely identical in the α-helix region. The only difference in the loop is a conservative mutation of Ile11 to Val11 in lucifensin. Furthermore, as Asp4 and Arg23 also are conserved in lucifensin, it supports that membrane pore formation may be a possible mechanism of antimicrobial activity for lucifensin.

However, a different study demonstrated that lucifensin and the fungal defensin plectasin each form an equimolar stoichiometric complex with the cell wall precursor lipid II (Schneider et al. 2010). NMR experiments showed that plectasin binds to a membrane-mimicking micelle of DPC (dodecylphosphocholine), and that the micelle bound plectasin further binds lipid II. Interestingly, plectasin did not exhibit the rapid lytic behavior expected from membrane channel formers, but instead showed a killing kinetics as determined via timekill assay, similar to cell wall synthesis interfering agents (Schneider et al. 2010). The lack of membrane channel forming ability of plectasin was further corroborated by potassium efflux experiments.

This difference in mechanism of action can be explained from the structure and sequence alignment: plectasin does not contain amino acids equivalent to Asp4 and Arg23, the residues essential for membrane channel formation of

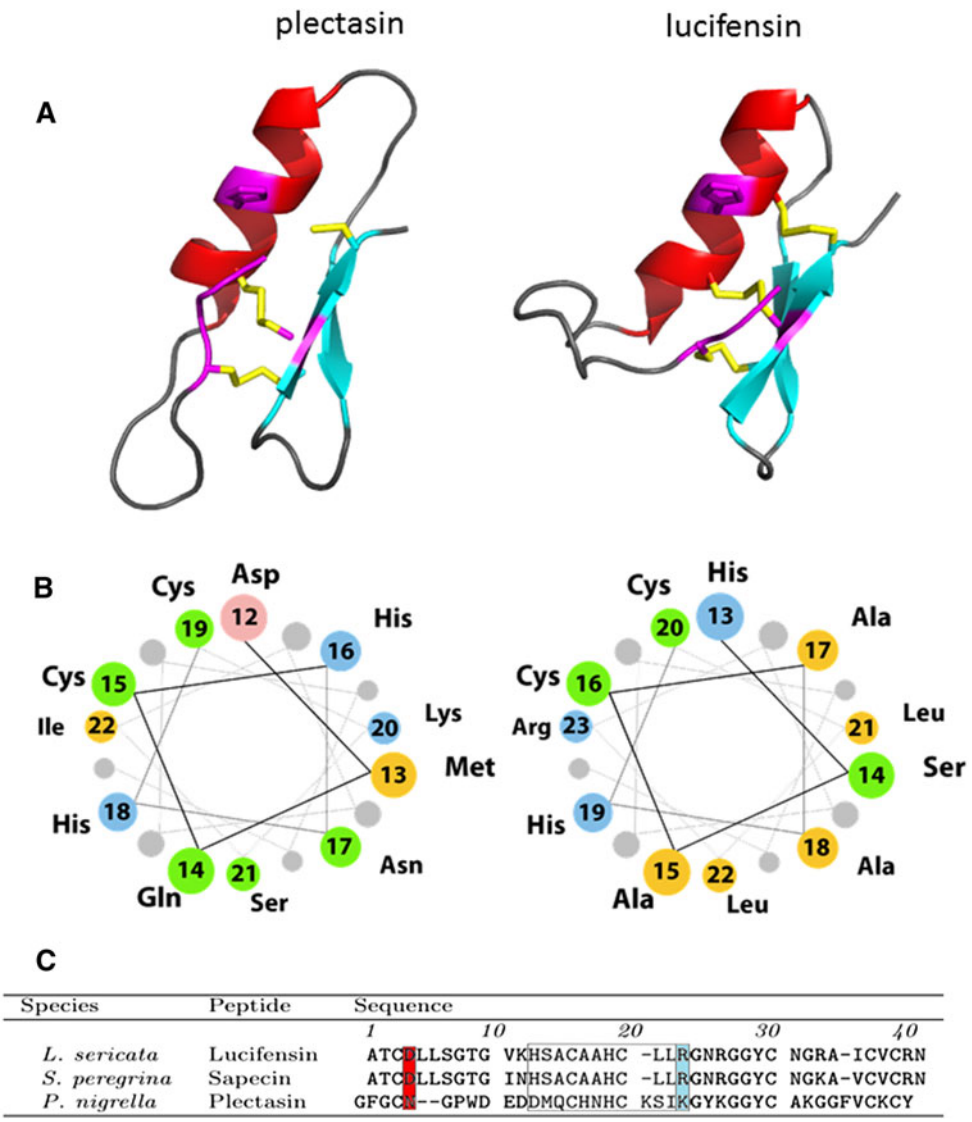


**Fig. 3** Comparison of lucifensin with plectasin: **a** structure with lowest energy in cartoon representation. Amino acids important for lipid II binding in plectasin (*left*) are shown in magenta (G1, F2,G3, C4, H18 and C37). The corresponding residues in lucifensin (*right*) are (A1, T2, C3, H19 and C36). The side chains are only shown for the two histidines, reflecting the fact that only H18 was proposed to bind with a side chain atom. **b** Helical wheel projection of the helices of plectasin (*left*) and lucifensin and sapecin (*right*) showing the difference in hydrophobicity of the solvent exposed part of the α-helix. **c** Sequence alignment of lucifensin, sapecin and plectasin highlighting the residues D4 and R23 and the α-helix (*box*) important for membrane pore formation

sapecin, at comparable positions in the sequence (Fig. 3). Furthermore, plectasin lacks most of the hydrophobic amino acids at the surface exposed side of the α-helix, that are thought responsible for the hydrophobic α-helix of sapecin being buried in the phospholipid membrane. When examining the α-helical wheel projection of plectasin and sapecin (Fig. 3), it is evident that plectasin only has one hydrophobic residue facing away from the cystines, whereas sapecin has 5. Further, although plectasin on the one hand and lucifensin and sapecin on the other hand have near-identical folding motifs, their sequence similarity is low (27.5% between plectasin and lucifensin and 30.0% between plectasin and sapecin).

As lucifensin also has the ability to form a complex with the cell wall precursor lipid II, it is possible that it has two mechanisms of antimicrobial activity. In the study of plectasin, an NMR based model of the plectasin-lipid II complex was presented (Schneider et al. 2010). In this model the pyrophosphate moiety forms hydrogen bonds to Phe2, Gly3, Cys4, and Cys37, and the D-γ-glutamate of Lipid II forms a salt bridge with the N terminus of plectasin and the sidechain of His18. Lucifensin also contains a histidine (His 19) at the equivalent position of the structure. The N-terminal residues of plectasin, which were also involved in lipid II binding, are, however, not conserved in lucifensin.

The N-terminal part of the sequence is highly conserved between lucifensin and other insect defensins (Bulet et al. 1992). Furthermore, the spatial location of histidine 18 (or equivalent position) in the α-helix of lucifensin and plectasin are also highly conserved throughout the insect defensins. Therefore, it is likely that many insect defensins, including lucifensin, have both the bacterial membrane and lipid II as targets for their antimicrobial activity.

**Acknowledgments** The project is part of the DanCARD center funded by the Danish Council for Strategic Research. We would like

to acknowledge the Carlsberg Research Center for use of the 800 MHz spectrometer and in that respect thank Bent Pedersen and Sebastian Meier for technical assistance with recording of the NMR spectra. We would also like to thank Charlotte Steen for aiding with MALDI-TOF MS. The NMR laboratory at Aalborg University is supported by the Obel and SparNord foundations. Discovery and recombinant production of Lucifensin was supported by a grant from the Danish Research Council for Technology and Production (grant number 274-05-0435 to K. A. K).

## References

Andersen AS, Sandvang D, Schnorr KM, Kruse T, Neve S, Joergensen B, Karlsmark T, Krogfelt KA (2010) A novel approach to the antimicrobial activity of maggot debridement therapy. J Antimicrob Chemother 65(8):1646–1654

Bulet P, Cociancich S, Reuland M, Sauber S, Bischoff R, Hegy G, Van Dors-selaer A, Hetru C, Hoffmann JA (1992) A novel insect defensin mediates the inducible antibacterial activity in larvae of the dragon fly *Aeschna cyanea* (Paleoptera, odonata). Eur J Biochem 209(3):977–984

Čeřovský V, Žďárek J, Fučík V, Monincová L, Voburka V, Bém R (2009) Lucifensin, the long-sought antimicrobial factor of medicinal maggots of the blowfly *Lucilia sericata*. Cell Mol Life Sci 67(3):455–466

Cociancich S, Ghazi A, Hetru C, Hoffmann JA, Letellier L (1993) Insect defensin, an inducible antibacterial peptide, forms voltage-dependent channels in *Micrococcus luteus*. J Biol Chem 268(26):19239–19245

Cornet B, Bonmatin J, Hetru C, Hoffmann JA, Ptak M, Vovelle F (1995) Refined three-dimensional solution structure of insect defensin A. Structure 3(5):435–448. PDB entry: 1ICA

Dumville JC, Worthy G, Bland JM, Cullum N, Dowson C, Iglesias C, Mitchell JL, Nelson EA, Soares MO, Torgerson DJ, VenUS II Team (2009) Larval therapy for leg ulcers (VenUS II): randomised controlled trial. BMJ 338:b773

Essmann U, Perera L, Berkowitz ML, Darden T, Lee H, Pedersen LG (1995) A smooth particle mesh Ewald method. J Chem Phys 103(19):8577

Hanzawa H, Shimada I, Kuzuhara T, Komano H, Kohda D, Inagaki F, Natori S, Arata Y (1990) $^{1}$H nuclear magnetic resonance study of the solution conformation of an antibacterial protein, sapecin. FEBS Lett 269:413-420. PDB entry: 1L4 V

Jaklic D, Lapanje A, Zupancic K, Smrke D, Gunde-Cimerman N (2008) Selective antimicrobial activity of maggots against pathogenic bacteria. J Med Microbiol 57(Pt 5):617–625

Keller R (2004) The computer aided resonance assignment tutorial, 1st edn. CANTINA Verlag, Goldau (Switzerland)

Kerridge A, Lappin-Scott H, Stevens JR (2005) Antibacterial properties of larval secretions of the blowfly, *Lucilia sericata*. Med Vet Entomol 19:333–337

Konagurthu AS, Whisstock JC, Stuckey PJ, Lesk AM (2006) MUSTANG: a multiple structural alignment algorithm. Proteins 64:559–574

Krieger E, Koraimann G, Vriend G (2002) Increasing the precision of comparative models with YASARA NOVA—a self-parameterizing forcefield. Proteins 47:393–402

Krieger E, Joo K, Lee J, Lee J, Raman S, Thompson J, Tyka M, Baker D, Karplus K (2009) Improving physical realism, stereochemistry and side-chain accuracy in homology modeling: four approaches that performed well in CASP8. Proteins 77(9): 114–122

Laskowski R, Rullmann J, MacArthur M, Kaptein R, Thornton J (1996) AQUA and PROCHECK-NMR: programs for checking the quality of protein structures solved by NMR. J Biomol NMR 8(4):477–486

López-Méndez B, Güntert P (2006) Automated protein structure determination from NMR spectra. J Am Chem Soc 128:13112–13122

Mygind PH, Fischer RL, Schnorr KM, Hansen MT, Sönksen CP, Ludvigsen S, Raventós D, Buskov S, Christensen B, De Maria L, Taboureau O, Yaver D, Elvig-Jørgensen SG, Sørensen MV, Christensen BE, Kjaerulff S, Frimodt-Moller N, Lehrer RI, Zasloff M, Kristensen HH (2005) Plectasin is a peptide antibiotic with therapeutic potential from a saprophytic fungus. Nature 437(7061):975–980

Schneider T, Kruse T, Wimmer R, Wiedemann I, Sass V, Pag U, Jansen A, Nielsen AK, Mygind PH, Raventos DS, Neve S, Ravn B, Bon-vin AMJJ, De Maria L, Andersen AS, Gammelgaard LK, Sahl H, Kristensen H (2010) Plectasin, a fungal defensin, targets the bacterial cell wall precursor lipid II. Science 328:1168–1172

Shen Y, Delaglio F, Cornilescu G, Bax A (2009) TALOS+: a hybrid method for predicting protein backbone torsion angles from NMR chemical shifts. J Biomol NMR 44(4):213–223

Takeuchi K, Takahashi H, Sugai M, Iwai H, Kohno T, Sekimizu K, Natori S, Shimada I (2004) Channel-forming membrane permeabilization by an antibacterial protein, sapecin. J Biol Chem 279: 4981–4987